Stimuli-Responsive Polymers. 5. Azobenzene Modified Polyaramides Containing Atropisomeric Binaphthyl Linkages: Tuning Chiroptical Behavior with Light and Heat

Steven R. Lustig,[†] Gerry J. Everlof,[‡] and Gary D. Jaycox*[,†]

DuPont Central Research and Development and DuPont Pharmaceuticals, Experimental Station, Wilmington, Delaware 19880-0328

Received August 8, 2000; Revised Manuscript Received January 17, 2001

ABSTRACT: Azobenzene modified polyaramides and several model compounds fitted with atropisomeric 2,2′-binaphthyl linkages exhibit thermo- and photoresponsive chiroptical behavior when evaluated in dilute solution environments. The *trans*-azobenzene modified polymers were characterized by CD spectra with intense molar ellipticities in the 300−400 nm spectral window. Specific rotation magnitudes at the sodium D-line ranged into the hundreds of degrees and were dependent upon the extent of binaphthyl loading along the polymer chain. The irradiation of the polymer samples to drive the *trans* → *cis* isomerization process resulted in an immediate chiroptical response, with CD band intensities and optical rotations significantly diminished. These effects were fully reversible and were attributed to the presence of one-handed helical conformations in the *trans*-azobenzene modified polymers that were severely disrupted following the *trans* → *cis* isomerization reaction.

Introduction

Photo- and thermoregulated conformational changes in azobenzene modified polymers provide an opportunity for the rational design of "smart" materials systems. Particularly noteworthy in this regard have been attempts to utilize local *trans*−*cis* isomerization reactions to induce well-defined conformational transitions in macromolecules endowed with main chain or pendent side chain azobenzene groups. Light-driven α-helix ↔ random coil, α-helix ↔ *β*-helix, and right helix ↔ left helix transitions in azobenzene modified polypeptides have been extensively investigated by Ueno[1,2] and Ciardelli.[3−5] More recently, Zentel and co-workers[6,7] have reported on a series of photomediated helix inversions in polyisocyanates that have been fitted with small quantities of chiral azobenzene side groups.

As depicted schematically in Scheme 1, the *trans*−*cis* isomerization reactions triggered within these helical polymers can ultimately give rise to twin photochromic and chiroptical responses that are intimately related. The nature of this interrelationship can often be fine-tuned by adjusting a number of parameters including polymer backbone structure, the location and extent of azobenzene loading, solvent type, and solution pH. Materials of this kind offer considerable insight into a variety of photomodulated biological processes, and they may be well-suited for optical data storage, polymeric sensory devices, and other technological applications.[5]

In an effort to construct high-performance materials endowed with stimuli-responsive chiroptical behavior, we have recently prepared a series of azobenzene modified polymers and related model compounds that are fitted with axially asymmetric *R*- or *S*-binaphthyl groups (Scheme 2). As was reported earlier, these film forming materials are amorphous, highly tractable, and thermally stable at temperatures exceeding 400 °C.[8,9] A number of these constructs adopt single-handed helical geometries in solution that are strongly per-

Scheme 1. Coupled Photochromic and Chiroptical Responses in Azobenzene Modified Helical Polymers

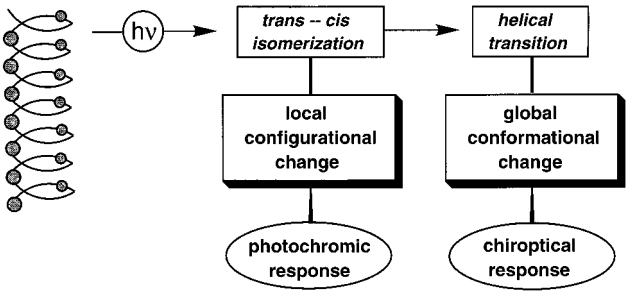

Scheme 2. Azobenzene Modified Polymers *trans*-1(R) and *trans*-1(S)−6

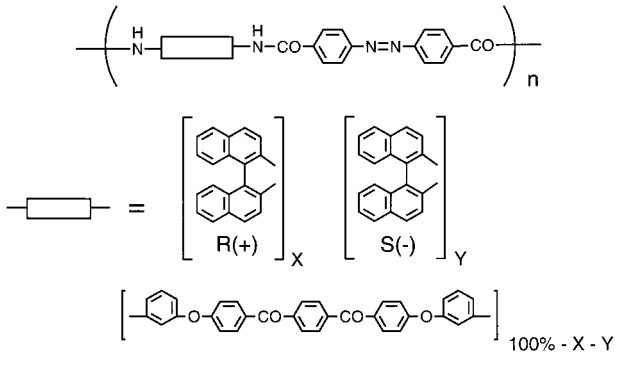

polymer	X (%)	Y (%)
1(R)	100	0
1(S)	0	100
2(S)	0	80
3(S)	0	60
4(S)	0	40
5(S)	0	20
6	0	0

[†] DuPont Central Research and Development.
[‡] DuPont Pharmaceuticals.
* To whom correspondence should be addressed. E-mail gary.d.jaycox@usa.dupont.com.

10.1021/ma001393p CCC: $20.00
Published on Web 02/20/2001

turbed by the *trans*−*cis* isomerization reaction. Herein, we demonstrate that light and heat can be effectively used to tune the chiroptical properties exhibited by this new polymer family.

Experimental Section

Materials. Anhydrous *N*,*N*-dimethylacetamide (DMAC) and methyl sulfoxide (DMSO) (Aldrich) were stored under Ar over 4A molecular sieves. *R*-(+)- and *S*-(−)-1,1′-binaphthyl-2,2′-diamine (99%, 99% ee, Aldrich) were both recrystallized from warm methanol and then rigorously dried in vacuo before use. All other reagents and solvents (>97%) were obtained from Aldrich and were used without further purification.

Polymer Syntheses. The *trans*-azobenzene modified polymers were prepared in the absence of room light by a series of low-temperature solution polycondensation reactions as described previously. [8,9]

Model Compound Synthesis. *Bis-amide from S-(−)-1,1′-Binaphthyl-2,2′-diamine and Benzoyl Chloride* (**7(S)**). To a magnetically stirred solution of *S*-(−)-1,1′-binaphthyl-2,2′-diamine (0.50 g, 1.76 mmol) in DMAC (20 mL) was slowly added benzoyl chloride (0.51 g, 3.63 mmol). After the addition was complete, the reaction mixture was warmed to 35−40 °C for 2 h and then cooled to room temperature. The resulting solution was poured into water (200 mL), giving a tan precipitate. The solid was collected by filtration and then dissolved into ethyl ether (75 mL) and extracted with water (3 × 50 mL) and brine (50 mL). The organic phase was concentrated in vacuo, giving **7(S)** (87%) as a light tan crystalline solid; mp 187−189 °C. ^{1}H NMR (DMSO-d_6, 500 MHz): δ 9.91 (s, 2 H), 8.10−8.15 (m, 2 H), 7.99−8.04 (m, 2 H), 7.84−7.90 (m, 2 H), 7.41−7.55 (m, 8 H), 7.29−7.38 (m, 6 H), 7.02−7.08 (m, 2 H). MS (K^+IDS): *m/e* 531 ([M]K^+); $[\alpha]^{25}_D$ = (−) 56.9 (*c* = 0.021 g/dL, THF). Anal. Calcd for $C_{34}H_{24}N_2O_2$: C, 82.91; H, 4.91; N, 5.69. Found: C, 82.88; H, 4.73; N, 5.98.

Bis-amide from R-(+)-1,1′-Binaphthyl-2,2′-diamine and Benzoyl Chloride (**7(R)**). This model compound was prepared in 89% yield from *R*-(+)-binaphthyl-2,2′-diamine and benzoyl chloride using the same procedure described above for model **7(S)**; mp 188−191 °C (lit.[10] mp 190 °C). ^{1}H NMR (DMSO-d_6, 500 MHz): δ 9.91 (s, 2 H), 8.11−8.16 (m, 2 H), 7.99−8.03 (m, 2 H), 7.84−7.91 (m, 2 H), 7.42−7.56 (m, 8 H), 7.29−7.39 (m, 6 H), 7.03−7.09 (m, 2 H). MS (K^+IDS): *m/e* 531 ([M]K^+); $[\alpha]^{25}_D$ = (+) 55.8 (*c* = 0.016 g/dL, THF). Anal. Calcd for $C_{34}H_{24}N_2O_2$: C, 82.91; H, 4.91; N, 5.69. Found: C, 83.05; H, 4.99; N, 5.60.

Bis-amide from S-(−)-1,1′-Binaphthyl-2,2′-diamine and 4-(Phenylazo)benzoyl Chloride (*trans*-**8(S)**). To a magnetically stirred solution of *S*-(−)-1,1′-binaphthyl-2,2′-diamine (1.00 g, 3.52 mmol) in DMAC (35 mL) was slowly added 4-(phenylazo)-benzoyl chloride (1.73 g, 7.07 mmol). After the addition was complete, the reaction mixture was stirred in the dark at room temperature for 8 h. The resulting solution was poured into water (150 mL), giving an orange precipitate. The solid was collected by filtration and then dissolved into chloroform (100 mL) and extracted with water (3 × 50 mL) and brine (50 mL). The organic phase was concentrated in vacuo, giving *trans*-**8(S)** (89%) as a bright orange foam: mp 135−140 °C. ^{1}H NMR (DMSO-d_6, 500 MHz): δ 10.10 (s, 2 H), 8.14−8.18 (d, 2 H), 8.00−8.08 (d, 2 H), 7.74−7.95 (m, 7 H), 7.59−7.64 (m, 3 H), 7.48−7.53 (m, 2 H), 7.31−7.38 (m, 2 H), 7.08−7.12 (d, 2H). MS (K^+IDS): *m/e* 739 ([M]K^+); $[\alpha]^{25}_D$ = (+) 208.1 (*c* = 0.021 g/dL, THF). Anal. Calcd for $C_{46}H_{32}N_6O_2$: C, 78.84; H, 4.60; N, 11.99. Found: C, 78.63; H, 4.61; N, 12.12.

Bis-amide from R-(+)-1,1′-Binaphthyl-2,2′-diamine and 4-(Phenylazo)benzoyl Chloride (*trans*-**8(R)**). This model compound was prepared in 91% yield from *R*-(+)-binaphthyl-2,2′-diamine and 4-(phenylazo)benzoyl chloride using the same procedure described above for model *trans*-**8(S)**; mp 136−141 °C. ^{1}H NMR (DMSO-d_6, 500 MHz): δ 10.11 (s, 2 H), 8.12−8.19 (d, 2 H), 8.01−8.08 (d, 2 H), 7.74−7.97 (m, 7 H), 7.58−7.63 (m, 3 H), 7.48−7.54 (m, 2 H), 7.31−7.39 (m, 2 H), 7.08−7.11 (d, 2H). MS (K^+IDS): *m/e* 739 ([M]K^+); $[\alpha]^{25}_D$ = (−) 205.3 (*c* = 0.020 g/dL, THF). Anal. Calcd for $C_{46}H_{32}N_6O_2$: C, 78.84; H, 4.60; N, 11.99. Found: C, 78.77; H, 4.59; N, 12.08.

General Methods. Melting points were determined in open capillary tubes with a Laboratory Devices (Holliston, MA) Mel-Temp unit and are uncorrected. A heating rate of 2 °C/min was consistently employed. Routine proton nuclear magnetic resonance (^{1}H NMR) spectra were obtained at 500 MHz on a Bruker Avance DRX-500 instrument. Tetramethylsilane was employed as a standard. Variable temperature ^{1}H NMR measurements were acquired in DMSO-d_6 at 500 MHz on a Varian Unity-Plus spectrometer. Peak positions are reported relative to the DMSO solvent peak at 2.50 ppm. UV−vis spectra were obtained with a Hewlett-Packard 8453 UV−vis spectrophotometer. Potassium ionization of desorbed species mass spectroscopy (MS K^+IDS) was performed on a Finnigan 4615B quadrupole GC/MS system. Elemental analyses were provided by Galbraith Laboratories (Knoxville, TN).

Inherent viscosity measurements were obtained in sulfuric acid at 25 °C with a polymer concentration of 0.5 wt %. Gel permeation chromatography (GPC) was carried out with a Waters HPLC 150C equipped with a refractive index detector. Polymer samples were dissolved into DMAC containing trace amounts of Ionol (antioxidant) and toluenesulfonic acid. Measurements were run at 135 °C, and narrow molecular weight polystyrene standards were employed for the purposes of GPC calibration.

Specific rotations, reported as deg dm^{-1} g^{-1} cm^3, were evaluated at the sodium D-line (589 nm) with a Perkin-Elmer model 341 polarimeter. Samples were dissolved in either tetrahydrofuran (THF) or DMAC. A thermostated 10 cm path length cell was utilized for all measurements. Circular dichroism (CD) spectra were obtained with a Jasco J600 spectropolarimeter fitted with a 450 W xenon arc lamp as a light source. Sample concentrations were typically on the order of 5×10^{-5} M, and data are given as deg cm^2 $dmol^{-1}$. All circular dichroism measurements were carried out in THF at room temperature unless otherwise indicated.

Low-intensity UV irradiations of polymer solutions were performed with a Black-Ray long wavelength UV lamp (San Gabriel, CA; model B 100 AP) with a maximum intensity centered near 360 nm. When desired, higher intensity UV irradiations were effected with a 450 W medium-pressure quartz mercury arc (Ace-Hanovia, Vineland, NJ; model 7883-14) equipped with a model 7830-60 power source. The lamp was fitted with an aluminum reflector having a reflectivity of 85%. Lamp-to-sample path length was typically 10 cm. A combination of optical cut-on and band-pass filters (Oriel Corp., Stratford, CT) were employed to furnish radiation within a desired spectral window.

CPK (Corey−Pauling−Koltun) and force field molecular modeling techniques were both employed in this study. All CPK techniques were based on the hard-sphere, excluded-volume, and freely rotating bond approximations. More detailed, realistic atomic interactions were obtained using classical force field molecular modeling. Force field molecular modeling was performed with the Compass force field[11−15] implemented by Cerius2 Version 4.0 and Discover Version 98.0 (Molecular Simulations Inc., San Diego, CA) software. Since detailed descriptions of the Compass force field are provided elsewhere,[11−15] only a terse overview is provided herein. It is most appropriate to use this force field and molecular mechanics methods when emphasizing the properties of large molecules, of molecules in condensed phases, and for properties that do not require the details of electron distributions. The Compass force field provided an empirical set of formulas to mimic interatomic interactions. The functional forms used in this force field included harmonic, anharmonic, and cross-coupling valence bonding terms for bond lengths, bond angles, torsion angles, and out-of-plane angles. Furthermore, the force field included nonbonded interactions such as van der Waals and Coulombic interactions. The assignment of specific parameters used to compute these interaction terms from geometric distances and angles was based on classifying atoms in different chemical environments into different "atom types". The force field provides a means to evaluate the potential energy of a molecular model in a given conformation. We employed standard Monte Carlo and minimization techniques

Table 1. Polymer Composition, Inherent Viscosity, and Molecular Weight Data

polymer (*trans*)	wt % azobenzene	wt % binaphthyl	η_{inh} (dL/g)[a]	M_n[b]	M_w/M_n[b]
1(R)	34.8	48.7	0.42	30 100	2.31
1(S)	34.8	48.7	0.35	27 800	2.15
2(S)	32.1	35.9	0.64	61 000	2.26
3(S)	29.8	25.0	0.53	59 400	2.18
4(S)	27.8	15.6	0.85	73 900	2.09
5(S)	26.1	7.3	1.16	74 800	2.22
6	24.5	0	1.77	80 400	2.30

[a] Determined in H_2SO_4 (0.5 wt %) at 25.0 °C. [b] Determined by GPC in DMAC at 135 °C.

within the Cerius2 software to search the space of conformations and to locate structures that possessed a conformational potential energy minimum.

Results and Discussion

The *trans*-azobenzene modified polymers shown in Scheme 2 were prepared earlier[8,9] from their respective monomers by a series of low-temperature solution polycondensation reactions carried out in DMAC. Unless otherwise indicated, polymer solutions were manipulated in the absence of room light to avoid the premature isomerization of the internal *trans*-azobenzene linkages. Backbone compositions, inherent viscosities, and molecular weight values determined for these materials are provided in Table 1 for comparison. Azobenzene contents ranged from about 25 to 35 wt % while chiral binaphthyl loadings in the polymer backbones varied more broadly, approaching nearly 49 wt % for polymers **1(R)** and **1(S)**. For this polymer series, inherent viscosities evaluated in H_2SO_4 trended downward with increasing binaphthyl monomer contents. Most of the *trans*-azobenzene modified polymers possessed moderately high molecular weights as evidenced by a series of GPC analyses carried out in DMAC. However, the number-average molecular weight values recorded for *trans*-**1(R)** and *trans*-**1(S)** were reduced by about a factor of 2 when compared to most of the other polymer variants fitted with lower levels of the atropisomeric binaphthyl linkage. These results may indicate that chain growth for **1(R)** and **1(S)** is hindered to some extent during the polycondensation reaction. Similar observations have been reported by Takeishi et al.[17] for other polyamides formed from 2,2′-linked binaphthyl monomers. The materials described herein were readily dissolved in DMAC and DMSO at room temperature. Importantly, polymer constructs fitted with higher levels of the kinked binaphthyl monomers were also soluble in a number of less aggressive, polar solvents including tetrahydrofuran (THF) and acetone.

All of these materials exhibited photo- and thermoregulated behavior in dilute solution consistent with the presence of multiple azobenzene chromophores or "stimuliphores" in their polymer backbones. Photoinduced *trans* → *cis* isomerization reactions were readily carried out by irradiating polymer solutions with filtered ($370 < \lambda < 400$ nm) ultraviolet light. This process typically afforded photostationary state compositions such that two out of every three azobenzene linkages assumed the higher energy *cis*-configuration. Activation energies for thermal "back"-reactions that restored the population of *trans*-azobenzene groups in the polymer chains were reported earlier.[8,9] These values fell near 21−22 kcal mol^{-1} when evaluated in THF or DMAC solvent media. Importantly, *cis*-isomer half-life values

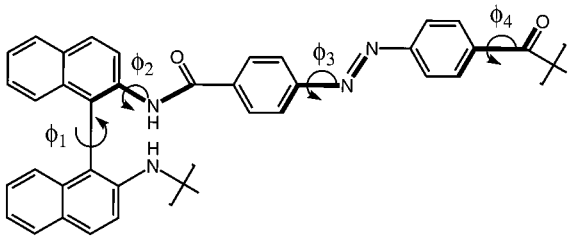

Figure 1. Torsional angles, ϕ_I, situated within the polymer backbone for *trans*-**1(R)** and *trans*-**1(S).**

at room temperature were greater than 1 day, enabling the acquisition of chiroptical data over short time periods that were uncomplicated by rapidly shifting *cis*−*trans* isomer ratios. When desired, thermally driven *cis* → *trans* return in these materials was greatly accelerated by warming the polymer solutions above room temperature. When carried out at 60 °C, nearly all of the more linear *trans*-azobenzene backbone linkages were restored in these systems within several hours. *Cis* → *trans* reorganization along the polyaramide backbone was also triggered photochemically by irradiating the polymer solutions with visible light for several minutes. This stimuli-responsive behavior was completely reversible over multiple cycles without any photodegradation or hysteresis effects.[18]

Molecular Modeling. In addition to impacting dilute solution viscosity and solubility behavior as described above, the placement of multiple *R*- or *S*-2,2′-linked binaphthyl units at regular intervals along a conformationally restricted polymer backbone can also lead to longer range helical order that is itself chiral.[17−19] For polymers *trans*-**1(R)** and *trans*-**1(S)**, the binaphthyl moieties present in the main chain are coupled through amide bonds to linear *trans*-azobenzene residues (Scheme 2). Here, the chiral 2,2′-binaphthyl linkages serve as helical directing groups, collectively projecting their axial asymmetries over the larger polyaramide backbone. CPK molecular modeling studies initially suggested that the two *trans*-azobenzene modified polymers could occupy distorted helical motifs with opposing screw directions. The putative helical geometries assigned to *trans*-**1(R)** and *trans*-**1(S)** were necessarily tied to a number of parameters, including the values selected for the dihedral angle spanning the twin naphthylene rings in each binaphthyl monomer unit. As reviewed recently by Pu,[19] both cisoid and transoid conformations are possible depending on the nature of the substituents appended to the 2- and 2′-positions of the binaphthyl ring system. The CPK models also indicated that the random inclusion of linear aryl ether ketone segments into the backbone of *trans*-**1(S)** would lead to further distortions in the helical geometries for variants **2(S)** through **5(S)**.

Force field modeling techniques afforded a number of refinements in the three-dimensional structures predicted for *trans*-**1(R)** and *trans*-**1(S)**. We were interested in understanding more precisely how longer range molecular order might arise within these conformationally restricted structures. Conformational analyses for the twin polymer systems are discussed in reference to Figure 1. Here, attention is focused on four separate torsional angles, designated ϕ_I, that are situated within the polyaramide backbone. Most notably, the dihedral angle (angle ϕ_1) within the binaphthyl group was found to have two minimum-energy torsional states, $g^{\pm}$, which stagger the twin naphthylene rings by

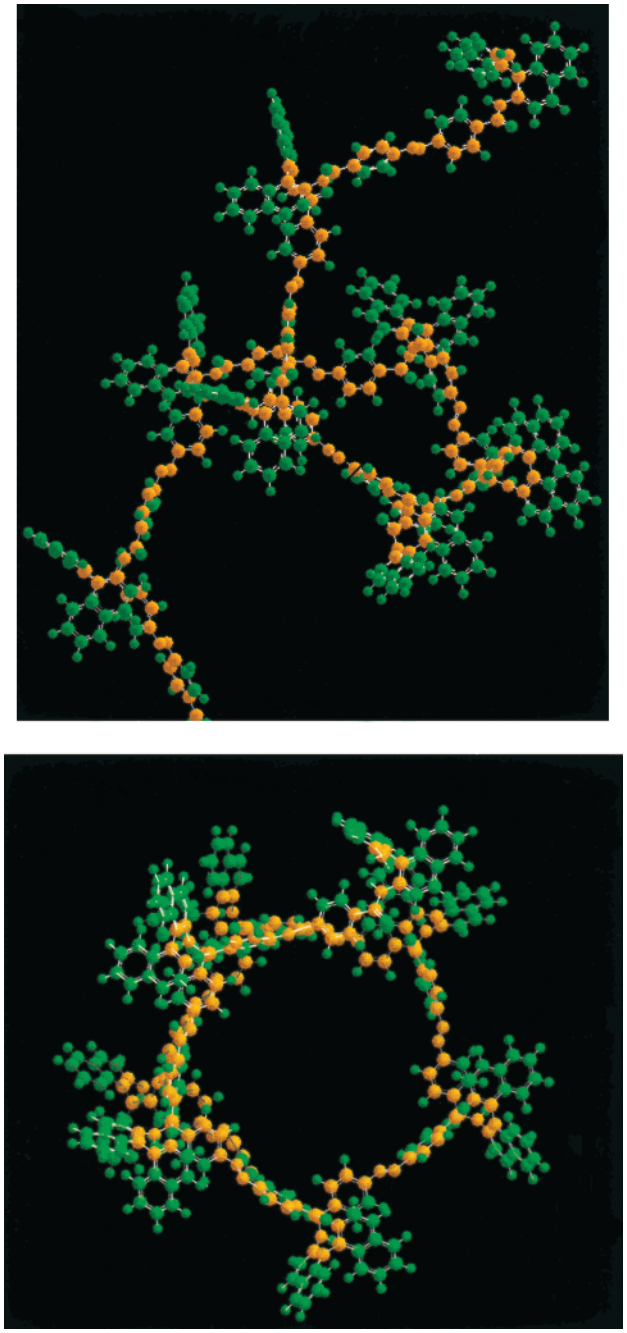

Figure 2. Computer-generated model for *trans*-**1(S)** showing a helical conformation predicted for this structure: (top) side view with helix axis diagonal to figure; (bottom) top view looking down helix axis. Atoms along the spine of the polymer backbone highlighted in orange.

(±)87°. In Figure 1, if the lower naphthylene ring is confined to the plane of the page, a positive angle conformation, g^+, will position the upper amide group below the plane of reference, giving an *S*-binaphthyl orientation. The binaphthyl bonding geometry within the polymer backbone creates a very large steric energy barrier, making $g^\pm$ transitions highly unlikely under the mild thermal conditions employed through out much of this study. Since the rest of the repeat unit also has restricted rotational isomeric states, a polymer chain comprised of *S*-binaphthyl linkages, e.g., *trans*-**1(S)**, will likely adopt the helical geometry shown in Figure 2 based on this current modeling scheme. For the lowest minimum-energy conformation determined thus far, ϕ_1 = (+)87° while ϕ_2 alternates between (+)88° and (−)-53° to permit intramolecular polar interactions between amide groups on opposite sides of the binaphthyl units. The helical geometry in Figure 2 appears to be stabilized by the Coulombic attraction between the amine hydrogen and the carbonyl oxygen in the amide groups on either side of each binaphthyl unit. Despite their close proximities, we hesitate to call these interactions formal hydrogen bonds because of the relatively wide angle between the amine and carbonyl bond vectors. In Figure 2 the torsion angle ϕ_3 alternates between (+)164° and (+)125° on each side of the azide bond with angle ϕ_4 alternating between (+)163° and (+)148° on each side of the azobenzene moiety to further assist in the aforementioned polar interactions. It should be understood that these interactions might easily be screened in polar solvents like DMAC and THF that were employed in this study. We have observed an ensemble of similar helical conformations that do not possess this particularly close polar interaction. These alternative conformations differ with respect to their helical unit heights and unit twists. We intend to present a more detailed account of these conformations in a forthcoming publication. In summary, the helical structures proposed for *trans*-**1(R)** and -**1(S)** appear to be propagated mainly due to the directionality of the intermonomer bonding in the chain and the dearth of alternative rotational isomeric states available for these particular sequences of monomers.

CPK molecular modeling also predicted that the chiral helical conformations occupied by the *trans*-polymers should be severely perturbed following the *trans* → *cis* isomerization reaction. Polymer geometries appear to collapse both on a local and on a more global scale, giving compact backbone structures. Similar predictions have been reported by Takeishi[20] for a related series of light-responsive polymers containing azobenzene main chain elements. The extent of this light induced conformational change will clearly depend on the *cis*-to-*trans* photostationary states reached within each polymer system. That the isomerization process can lead to significant changes in the conformational geometries and hydrodynamic volumes of azobenzene modified polymers has been experimentally confirmed in our own laboratory for a related family of stimuli-responsive materials.[21] A more quantitative assessment of the geometries that are likely to be adopted by *trans*-**1(R)** and *trans*-**1(S)** following the UV irradiation step will require further refinements in our molecular modeling procedures.

Circular Dichroism Measurements. Circular dichroism (CD) measurements were carried out in THF for a number of the polymers depicted in Scheme 2. Multiple CD spectra for *trans*-**1(R)** and for *trans*-**1(S)**−**4(S)** are overlaid in Figure 3 for comparison. A similar spectrum for variant **5(S)** fitted with only 7 wt % of the binaphthyl residue was not obtained because of its limited solubility in the THF solvent medium. As is readily apparent, *trans*-polymers **1(R)** and **1(S)** exhibited mirror-image behavior, each affording intense dichroic bands within the 280−400 nm spectral window. These bands stem from the *trans*-azobenzene $\pi-\pi^*$ transition and are clearly split into two distinct regions having both positive and negative amplitudes. The zero points falling at 338 nm in Figure 3 correspond to the wavelength where the *trans*-azobenzene stimuliphore exhibits a maximum in its optical absorbance spectrum. Bisignated or "split" dichroic spectra like those gathered

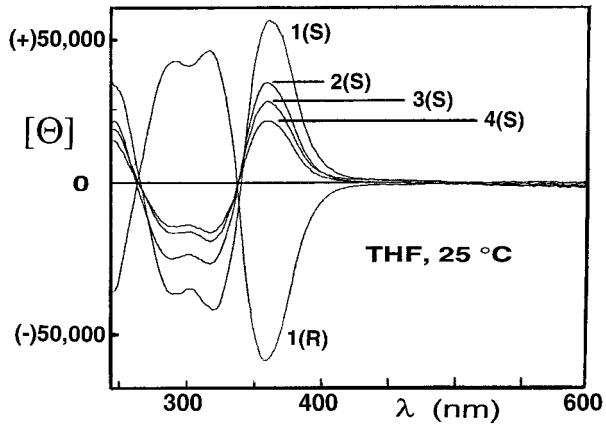

Figure 3. CD spectra for *trans*-**1(R)** and *trans*-**1(S)** through **4(S)** obtained in THF.

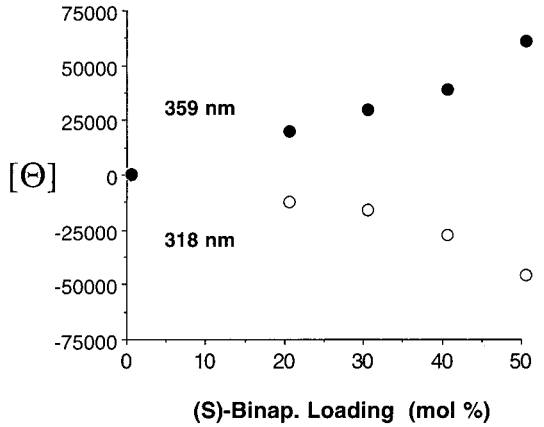

Figure 4. Molar ellipticity values for *trans*-**(S)** polymer series as a function of *S*-binaphthyl monomer loading. Data obtained at room temperature in THF.

here have been observed for a variety of azobenzene modified polymers that occupy one-handed helical geometries in solution.[17,20,22,23] This behavior has been attributed to exciton coupling that arises in response to chiral superstructures that localize two or more *trans*-azobenzene units in close proximity such that dipole−dipole interactions between chromophores become possible. That bisignated CD spectra were observed for polymers *trans*-**1(R)** and *trans*-**1(S)** is consistent with the presence of chiral backbone conformations predicted by the twin molecular modeling procedures detailed above.

trans-Azobenzene modified polymers **2(S)**−**4(S)** containing smaller populations of the chiral *S*-binaphthyl residue afforded qualitatively similar CD line shapes in THF when compared to *trans*-**1(S)**. However, as apparent from the plot provided in Figure 4, the CD band intensities for each of these polymers did not scale linearly with binaphthyl backbone content. More specifically, the magnitudes of the molar ellipticity extrema centered at 318 and 359 nm appeared to trend increasingly upward with higher mole percent loadings of the axially asymmetric binaphthyl segment. Although the various polymeric constructs were not uniform with respect to their chain lengths, it is interesting to speculate that the trend depicted in Figure 4 *may* reflect the added contributions to chiroptical behavior that are brought about by the presence of one-handed helical conformations that develop along regions of the polymer backbone. Such global helical geometries should become increasingly prevalent as higher levels of the helicogenic

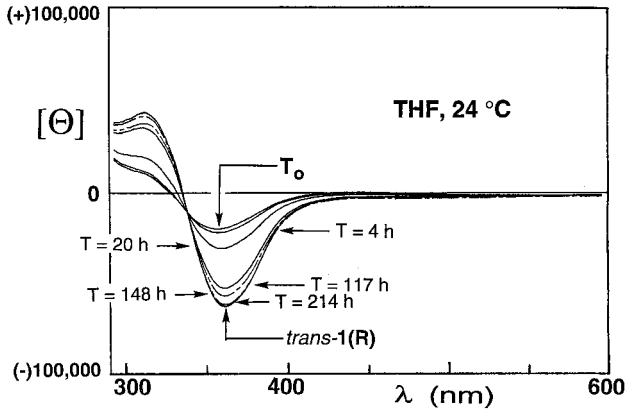

Figure 5. Time-resolved CD spectra for polymer **1(R)** acquired 0.5 (T_0), 4, 20, 117, 148, and 214 h after irradiation in THF. A CD plot for *trans*-**1(R)** is shown for comparison.

binaphthyl monomer are randomly incorporated into the polymer chain.

The exposure of the polymer solutions to filtered ($370 < \lambda < 400$ nm) UV light to drive the *trans* → cis isomerization reaction produced an immediate change in the behavior of these materials. Notably, CD band intensities for all of the samples were significantly diminished within the 280−400 nm spectral region. A CD spectrum for polymer **1(R)** having a light-induced *cis*-to-*trans* photostationary state near 65:35 is provided in Figure 5 (plot T_0). Here, the molar ellipticity values for the twin extrema located at 318 and 359 nm were reduced by a factor of 3 following the illumination step. As expected, this light-stimulated chiroptical response was completely reversible. Time-resolved spectra acquired at different intervals after the irradiation procedure are included in Figure 5 for a polymer solution that was stored in the dark at 24 °C. Importantly, a CD plot obtained after 214 h under these conditions was virtually identical to that recorded for the preirradiated polymer (plot *trans*-**1(R)**). The other azobenzene modified polymers described above exhibited similar behavior when evaluated in THF.

The reversible chiroptical response depicted in Figure 5 can be attributed to a combination of local and longer-range effects that are operative in these stimuli-responsive materials (Scheme 1). As indicated in Scheme 2, the main chain azobenzene groups in *trans*-**1(R)** are flanked to either side by neighboring chiral binaphthyl segments and thus reside locally in an asymmetric environment. From our molecular modeling efforts detailed above, it is plausible that this environment will be further influenced by the presence of longer-range helical backbone conformations that are also chiral. The light driven *trans* → *cis* isomerization reaction triggered within the polymer backbone will diminish the population of *trans*-azobenzene linkages that give rise to the $\pi-\pi^*$ band centered at 338 nm. This local photochromic response will significantly reduce the magnitude of the CD couplet appearing between 280 and 400 nm in Figure 5. At the same time, the isomerization process will also disrupt the global helical geometries adopted by the polymer backbone, potentially modifying further the CD spectrum for this polymer system. Because the light-induced *trans* → *cis* photoresponse does not lead to a 100% *cis*-state within the polymer, a fraction of the atropisomeric binaphthyl groups embedded in the polymer backbone will continue to be surrounded by *trans*-azobenzene moieties. Thus, the bisignated dichroic band

Table 2. Polymer Specific Rotation Values before (− *hν*) and after (+ *hν*) Near-UV Light Exposure Measured in THF and DMAC

		$[\alpha]^{25}_D$ (deg dm^{-1} g^{-1} cm^3)[a]			
		−*hν*		+*hν*[b]	
polymer	binaphthyl content by ^{1}H NMR (mol. %)	THF	DMAC	THF	DMAC
1(R)	50	(−) 530	(−) 488	(−) 46	(−) 146
1(S)	50	(+) 511	(+) 486	(+) 35	(+) 139
2(S)	40	(+) 335	(+) 388	(+) 30	(+) 107
3(S)	30	(+) 231	(+) 225	(+) 10	(+) 61
4(S)	20		(+) 158		(+) 40
5(S)	10		(+) 79		(+) 16
6	0		0		0

[a] Values typically ±1%. [b] Rotation data obtained within 30 min of light exposure.

shown in Figure 5 will not be completely eliminated from the CD spectrum following UV light exposure. Starting from the 65:35 *cis*-to-*trans* photostationary state reached in **1(R)**, a series of thermally mediated *cis* → *trans* relaxation steps within the polymer's main chain will simultaneously restore both the number of *trans*-azobenzene linkages and the helical conformations that they induce, thus reversing the chiroptical response shown in plot T_0 of Figure 5. That the CD plot obtained for **1(R)** after 214 h in the dark was nearly identical to the spectrum for the preirradiated polymer sample is consistent with a *cis*-azobenzene half-life near 60 h determined by optical absorbance spectroscopy under these experimental conditions.[9]

Optical Rotation Measurements. Macromolecules that adopt one-handed helical geometries often display large rotation magnitudes when evaluated in solution or in solid-state environments. D-line specific rotations ranging into the hundreds or even thousands of degrees have been recorded for a number of chiral helical polymers [24,25] prepared via helix-sense selective polymerization techniques, including polychloral,[26,27] various poly(trityl methacrylate)s,[28,29] and poly(isocyanide)s.[30,31] Other helical structures including novel helicene oligomers constructed from six or more fused aromatic rings also display exceptionally high optical rotation magnitudes in solution which derive from their chiral, conformationally rigid molecular frameworks.[32]

For the binaphthyl-containing polymers described in this study, additional insight into the nature of their stimuli-responsive chiroptical properties was gained by carrying out optical rotation measurements in both THF and the more polar solvent, DMAC. When centered at the sodium D-line (589 nm), these measurements were well removed from the strong $\pi-\pi^*$ and much weaker $n-\pi^*$ azobenzene transitions residing within the polymer backbones. As expected, polymers *trans*-**1(R)** and *trans*-**1(S)** each exhibited enhanced optical rotatory power in THF, with D-line specific rotations falling near (−)530 and (+)511 deg dm^{-1} g^{-1} cm^3, respectively. Interestingly, the signs of the optical rotations recorded for these polymers were inverted with respect to those for their corresponding binaphthyl diamine building blocks. Rotation magnitudes for **1(R)** and **1(S)** were reduced by more than a factor of 10 when their THF solutions were briefly exposed to filtered UV light (Table 2). This behavior mirrors that described above for the circular dichroism measurements and is again consistent with the disruption of helical conformations along the polymer backbone that are triggered in response to the *trans* → *cis* isomerization reaction (see Scheme 1).

Specific rotation values gathered at the sodium D-line for the seven azobenzene modified polymers before and after illumination are displayed in Table 2 for comparison. Data are provided for both the THF and DMAC solvent systems for all cases where the polymers were sufficiently soluble. The optical rotation results summarized in Table 2 are interesting in a number of respects. In their preirradiated, *all-trans* states, the materials modified with atropisomeric binaphthyl units exhibited large specific rotations, with rotation magnitudes clearly trending upward with increasing *S*-binaphthyl backbone contents. Rotation values gathered in THF were slightly larger (within 7%) when compared to those obtained in DMAC. The illumination of these polymer solutions with filtered UV radiation produced a significant drop in their optical rotatory powers. However, this light induced drop was much less pronounced for the DMAC solvent system. For these materials, optical absorbance measurements coupled with ^{1}H NMR spectroscopic data have revealed that both *cis*−*trans* backbone compositions in the photostationary state, and *cis* → *trans* isomerization rates, are only slightly effected by the choice of solvent.[8,9] Therefore, the solvent dependent disparities in the rotation data for the illuminated samples cannot be attributed to radically different *cis-to-trans* isomeric ratios within the polymer backbones at the time of measurement. It is interesting to speculate that this behavior may reflect other kinds of conformational changes that occur within these materials that are dependent upon the polarity or the hydrogen bonding potential of the solvent medium. For example, it is well-known that the dipole moments measured for *trans*-4,4′-disubstitued azobenzenes increase dramatically during the light induced isomerization reaction.[33,34] With significant populations of the more polar *cis*-azobenzene linkage randomly dispersed along their main chains, the irradiated polymers may be more sensitive to differences in solvent polarities than their all *trans* counterparts. Experimental efforts designed to further test this notion are currently underway.

Specific rotation values for **1(S)** dissolved in DMAC were also tracked as a function of time following the irradiation procedure. Changes in this polymer's optical rotatory power were evaluated at three different isotherms for samples stored in the dark to promote the thermally mediated *cis* → *trans* 'back"-reaction. As indicated by the series of linear plots provided in Figure 6, the recovery of rotation magnitudes was clearly a first-order process characterized by a strong temperature dependence. Rate constants calculated for the restoration of optical activity in **1(S)** varied from 1.86 × 10^{-4} min^{-1} at 25 °C to a velocity nearly 65 times greater for the 60 °C isotherm. On the basis of these polarimetric data, an activation energy for this process was determined to lie near 23.5 kcal mol^{-1}. This value is in good accord with an activation energy determined for the *cis* → *trans* isomerization reaction by optical absorbance spectroscopy.[8,9] The azobenzene isomerization process predicted to restore helical backbone structure and the optical rotatory power exhibited by the polymer sample thus appear to be well correlated. This finding is fully consistent with our explanation posited above for the origins of chiroptical behavior in these stimuli-responsive materials.

Model Compound Studies. The two atropisomeric binaphthyl diamine monomers and a number of model

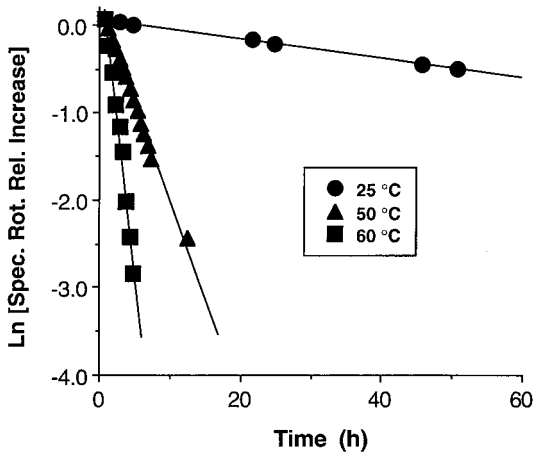

Figure 6. First-order plots for the "dark" recovery of $[\alpha]_D$ for polymer **1(S)**. Data are for three different isotherms in DMAC.

Scheme 3. Model Compounds 7(R), 7(S), *trans*-8(R), and *trans*-8(S)

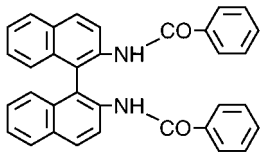

7(R) and 7(S)

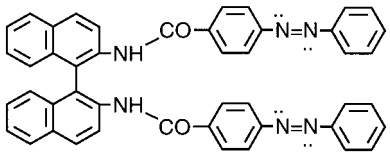

***trans*-8(R) and 8(S)**

compounds representing portions of the polymer backbone in **1(R)** and **1(S)** were also evaluated for their chiroptical behavior as part of this study. Derivatives **7(R)**, **7(S)**, **8(R)**, and **8(S)** shown in Scheme 3 were prepared by treating the corresponding binaphthyl diamine building blocks with either benzoyl chloride or 4-(phenylazo)benzoyl chloride in DMAC.

CD spectra for *trans*-**8(R)** and *trans*-**8(S)** acquired in THF are provided in Figure 7. As is immediately apparent, these bisignated plots bare a striking resemblance to the spectra displayed in Figure 3 for the *trans*-polymer samples. Like its polymeric analogue *trans*-**1(R),** model *trans*-**8(R)** exhibited a pronounced CD couplet with a negative first Cotton effect followed by a positive second Cotton effect appearing over shorter wavelengths. Predictably, the CD couplet recorded for the mirror-image isomer *trans*-**8(S)** was inverted within this spectral region. Falling near 328 nm, the zero points in both of these plots were blue-shifted by about 10 nm with respect to those for the polymer systems mentioned above. As expected, the twin model compounds dissolved in THF displayed absorbance maxima centered at 328 nm stemming from the $\pi-\pi^*$ transition for their *trans*-azobenzene chromophores. The irradiation of these solutions with filtered UV light produced an immediate change in their CD plots, with dichroic band intensities between 280 and 400 nm greatly reduced. As for the

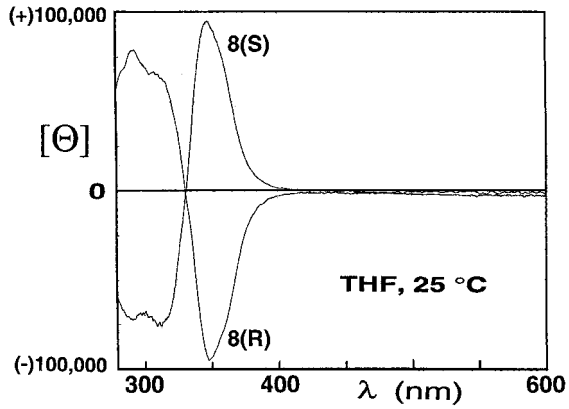

Figure 7. CD spectra for model compounds *trans*-**8(R)** and *trans*-**8(S)** in THF.

Table 3. Model Compound Specific Rotation Values before (−*hν*) and after (+*hν*) Near-UV Light Exposure Measured in THF

	$[\alpha]^{25}_D$ (deg dm^{-1} g^{-1} cm^3)	
compound	$-h\nu$	$+h\nu$[a]
R-(+)-1,1′-binaphthyl-2,2′-diamine	(+) 156	
7(R)	(+) 56	
8(R)	(−) 205	(+) 66
S-(−)-1,1′-binaphthyl-2,2′-diamine	(−) 155	
7(S)	(−) 57	
8(S)	(+) 208	(−) 69

[a] Rotation values measured within 30 min of light exposure.

stimuli-responsive polymers described earlier, these changes were completely reversible over time when tracked in the absence of light.

That the binaphthyl modified polymers and model compounds exhibited similar CD behavior was not unexpected. In both the high and low molecular weight constructs, the *trans*-azobenzene stimuliphores are anchored in chiral space by atropisomeric binaphthyl units, leading to exciton splitting in their respective CD plots. Upon illuminating these samples with UV light, the intense $\pi-\pi^*$ transition of the *trans*-azobenzene group will be severely diminished along with the intensities of the corresponding dichroic bands falling within this region of the spectrum. Importantly, these results suggest that the CD behavior recorded for the polymeric variants is largely dominated by the local chiral environments surrounding the main chain azobenzene stimuliphores present within these systems.

D-line specific rotations for the two binaphthyl diamine monomers and the four model compounds are summarized in Table 3. Here, a number of interesting comparisons can be made. When evaluated in THF, the *R*-(+)-1,1′-binaphthyl-2,2′-diamine building block exhibited a specific rotation near (+)156 deg dm^{-1} g^{-1} cm^3. The specific rotation magnitude measured for its bisbenzamide analogue **7(R)** was significantly reduced, falling by nearly a factor of 3. Capping the *R*-binaphthyl ring system with *trans*-azobenzene "arms" to mimic a larger fragment of the polymer backbone in *trans*-**1(R)** produced a new derivative *trans*-**8(R)** with a rotation of (−)205 deg dm^{-1} g^{-1} cm^3. This value compares to a specific rotation of (−)530 deg dm^{-1} g^{-1} cm^3 measured in THF for the larger polymer chain (Table 2). Both the *trans*-azobenzene modified model compound and its polymeric analogue exhibited levorotatory behavior in contrast to the positive rotations afforded by the *R*-binaphthyl diamine monomer and derivative **7(R)**. That

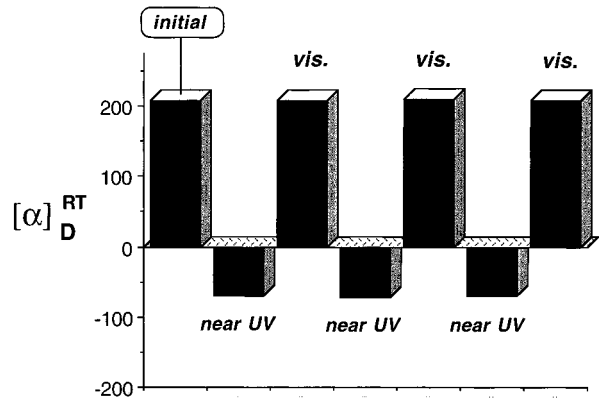

Figure 8. Photoregulated chiroptical switching for model compound **8(S)** in THF. Data for three complete UV−vis illumination cycles shown.

the optical rotatory power determined for polymer *trans*-**1(R)** exceeded that measured for its model compound *trans*-**8(R)** by a factor of 2.6 is strongly suggestive of the presence of higher structural order within the polymer backbone that is also chiral. As expected, similar trends in chiroptical behavior were noted for the *S*-(−)-1,1′-binaphthyl-2,2′-diamine building block and its related derivatives (Tables 2 and 3).

The specific rotation values for **8(R)** and **8(S)** dissolved in THF were also measured after the illumination step. As indicated in Table 3, the exposure of the twin model compounds to near-ultraviolet light resulted in an *inversion* of their relative signs of optical rotation. Rotation magnitudes were restored to their original values via thermally mediated or visible light-induced *cis* → *trans* isomerization processes. For species **8(S)**, light-triggered chiroptical switching between positive and negative rotations was carried out over multiple near-UV light−visible light irradiation cycles with no apparent loss of reversibility as depicted in Figure 8. *These model compounds thus join a unique class of materials that can be reversibly driven from one state to another in response to an applied stimulus.* Derivatives of this kind are increasingly viewed as attractive candidates for a variety of molecular device and optical data storage applications.[35] Species **8(R)** and **8(S)** along with several of their larger analogues are currently undergoing extensive evaluation in this regard.

It is interesting to note that the light-induced inversion of optical rotations observed for models **8(R)** and **8(S)** lies in stark contrast to the chiroptical behavior reported in Table 2 for the larger azobenzene modified polymer samples. To some degree, these results may stem from different *trans* → *cis* conversions for the low and high molecular weight constructs that sterically or electronically alter the value of the dihedral angle within the atropisomeric binaphthyl ring system. That changes in this rotational angle can impact the CD and optical rotation behavior of binaphthyl derivatives has been discussed in a number of earlier reports.[36−38] In our own laboratory, ^{1}H NMR measurements obtained in THF-d_8 immediately following the irradiation process have indicated that 90% of the azobenzene groups in model **8(R)** adopt the higher energy *cis*-configuration in response to UV light exposure. By comparison, the photostationary state achieved in polymer **1(R)** under identical conditions tended to be less enriched in the *cis*-isomer (ca. 65% *cis*), probably due to steric constraints imposed by the larger polymer chain.

Conclusions

Azobenzene modified polyaramides and several low-molecular-weight analogues fitted with atropisomeric 2,2′-binaphthyl linkages were shown to display thermo- and photoresponsive chiroptical behavior when evaluated in dilute solution environments. The *trans*-azobenzene modified polymers were predicted to occupy chiral helical geometries and were characterized by CD spectra with intense molar ellipticities in the 300−400 nm spectral window. CD plots were bisignated and exhibited both positive and negative Cotton effects. This behavior was consistent with exciton coupling between neighboring azobenzene chromophoric groups positioned in a chiral helical environment. Specific rotation magnitudes measured at the sodium D-line for these materials ranged into the hundreds of degrees and were found to be dependent upon the extent of binaphthyl loading along the polymer chain. The irradiation of the polymer samples with near-ultraviolet light to drive the *trans* → *cis* isomerization process resulted in an immediate chiroptical response, with CD band intensities and optical rotations significantly diminished. These effects were fully reversible and were attributed to the presence of one-handed helical conformations in the *trans*-azobenzene modified polymers that were severely disrupted following the *trans* → *cis* isomerization reaction.

Acknowledgment. G.D.J. thanks W. J. Simonsick, Jr. (DuPont Marshall R & D Laboratory), and R. Parisi for their assistance with the KIDS mass spectroscopy and NMR measurements reported herein. This paper is DuPont Contribution No. 8080 and is Part 5 in the series *Stimuli-Responsive Polymers*.

Supporting Information Available: An extensive table listing atomic coordinates for all atoms in the helical structure shown in Figure 2; data provided in the standard Protein Data Bank format. This material is available free of charge via the Internet at http://pubs.acs.org.

References and Notes

(1) Ueno, A.; Anzai, J.; Osa, T.; Kadoma, Y. *Bull. Chem. Soc. Jpn.* **1979**, *52*, 549.
(2) Ueno, A.; Takahashi, K.; Anzai, J.; Osa, T. *J. Am. Chem. Soc.* **1981**, *103*, 6410.
(3) Pieroni, O.; Houben, J. L.; Fissi, A.; Costantino, P.; Ciardelli, F. *J. Am. Chem. Soc.* **1980**, *102*, 5913.
(4) Fissi, A.; Pieroni, O.; Ciardelli, F. *Biopolymers* **1987**, *26*, 1993.
(5) Ciardelli, F.; Pieroni, O.; Fissi, A.; Carlini, C.; Altomare, A. *Br. Polym. J.* **1989**, *21*, 97.
(6) Maxein, G.; Zentel, R. *Macromolecules* **1995**, *28*, 8438.
(7) Muller, M.; Zentel, R. *Macromolecules* **1996**, *29*, 1609.
(8) Jaycox, G. D. *Polym. Prepr., Am. Chem. Soc., Div. Polym. Chem.* **1998**, *39* (2), 472.
(9) Howe, L. A.; Jaycox, G. D. *J. Polym. Sci., Polym. Chem. Ed.* **1998**, *36*, 2827.
(10) Schulz, R. C.; Jung, R. H. *Makromol. Chem.* **1968**, *116*, 190.
(11) Sun, H. *J. Phys. Chem. B* **1998**, *102*, 7338.
(12) Sun, H.; Rigby, D. *Spectrochim. Acta* **1997**, *53A*, 1301.
(13) Rigby, D.; Sun, H.; Eichinger, B. E. *Polym. Int.* **1997**, *44*, 311.
(14) Sun, H.; Ren, P.; Fried, J. R. *Comput. Theor. Polym. Sci.* **1998**, *8*, 229.
(15) Newsam, J. M.; Sun, H.; Rigby, D.; Eichinger, B. E.; Bick, A.; Freeman, C. M.; Gorman, A. M. Abstract no. COMP-096, *Book of Abstracts*, 217th American Chemical Society National Meeting, Anaheim, CA, March 21−25, 1999 (CODEN: 67GHA6 AN 1999: 146687).
(16) The Compass force field is currently a licensed product of Molecular Simulations, Inc., 9685 Scranton Road, San Diego, CA 92121 (http://www.msi.com).
(17) Kondo, F.; Takahashi, D.; Kimura, H.; Takeishi, M. *Polym. J.* **1998**, *30*, 161.

(18) Jaycox, G. D.; Everlof, G. J. *Polym. Prepr. (Div. Polym. Chem., Am. Chem. Soc.)* **1999**, *40* (1), 536.
(19) Pu, L. *Chem. Rev.* **1998**, *98*, 2405.
(20) Kondo, F.; Kakimi, S.; Kimura, H.; Takeishi, M. *Polym. Int.* **1998**, *46*, 339.
(21) Beattie, M. S.; Jackson, C.; Jaycox, G. D. *Polymer* **1998**, *39*, 2597.
(22) Angiolini, L.; Caretti, D.; Carlini, C.; Salatelli, E. *Macromol. Chem. Phys.* **1995**, *196*, 2737.
(23) Angiolini, L.; Caretti, D.; Giorgini, L.; Salatelli, E.; Altomare, A.; Carlini, C.; Solaro, R. *Polymer* **1998**, *39*, 6621.
(24) Vogl, O.; Jaycox, G. D.; Kratky, C.; Simonsick, Jr., W. J.; Hatada, K. *Acc. Chem. Res.* **1992**, *25*, 408.
(25) Okamoto, Y.; Nakano, T. *Chem. Rev.* **1994**, *94*, 349.
(26) Jaycox, G. D.; Vogl, O. *Polym. J.* **1991**, *23*, 1213.
(27) Jaycox, G. D.; Vogl, O. *Makromol. Chem., Rapid Commun.* **1990**, *11*, 61.
(28) Okamoto, Y.; Suzuki, K.; Ohta, K.; Hatada, K.; Yuki, H. *J. Am. Chem. Soc.* **1979**, *101*, 4763.
(29) Okamoto, Y.; Yashima, E.; Nakano, T.; Hatada, K. *Chem. Lett.* **1987**, 759.
(30) Nolte, R. J. M.; van Beijnen, A. J. M.; Drenth, W. *J. Am. Chem. Soc.* **1974,** *96*, 5932.
(31) Drenth, W.; Nolte, R. J. M. *Acc. Chem. Res.* **1979**, *12*, 30.
(32) Meurer, K. P.; Voegtle, F. Helical Molecules in Organic Chemistry. In *Topics in Current Chemistry*; Springer-Verlag: Berlin, 1985; Vol. 127, pp 32−57.
(33) Lang, J. J.; Robertson, J. M.; Woodward, I. *Proc. R. Soc. London, Ser. A* **1939**, *171*, 398.
(34) Kumar, G. S.; Neckers, D. C. *Chem. Rev.* **1989**, *89*, 1915.
(35) Feringa, B. L.; Huck, N. P. M.; Schoevaars, A. M. *Adv. Mater.* **1996**, *8*, 681.
(36) Mason, S. F.; Seal, R. H.; Roberts, D. R. *Tetrahedron* **1974**, *30*, 1671.
(37) Di Bari, L.; Pescitelli, G.; Salvadori, P. *J. Am. Chem. Soc.* **1999**, *121*, 7998.
(38) Di Bari, L.; Pescitelli, G.; Marchetti, F.; Salvadori, P. *J. Am. Chem. Soc.* **2000**, *122*, 6395.

MA001393P